

Magnetic-Field Scaling of Dimensionally Similar Tokamak Discharges

R. E. Waltz, J. C. DeBoo, and M. N. Rosenbluth^(a)

General Atomics, San Diego, California 92186-9784

(Received 9 August 1990)

Dimensionally similar tokamak discharges with all dimensionless parameters the same except the relative gyroradius can be scaled to ignition-regime discharges of larger size and/or field in analogy to the principles of wind tunnel design. This Letter describes the first controlled experiment to determine whether the scaling with relative gyroradius corresponds to short- or long-wavelength turbulence.

PACS numbers: 52.25.Fi, 52.30.-q, 52.55.Fa

A tokamak can operate in a variety of confinement regimes: low density, neo-Alcator, high-density Ohmic saturation, L -mode high-power heating, as well as H mode.¹ This suggests that there may be several transport mechanisms at work and, in particular, there may be separate central and edge mechanisms. Even if we understood these mechanisms better, modeling them in sufficient detail to describe even the global confinement time becomes very complex. However, we argue in this Letter that our lack of complete understanding does not prevent us from accurately scaling present tokamaks to ignition devices of larger radial size (a) and magnetic-field strength (B) provided we apply our most basic knowledge of the dimensional constraints on diffusive transport mechanisms. We will show that by keeping all dimensionless parameters constant except the relative ion gyroradius, it should be possible to map existing discharges in any of the operating regimes into "dimensionally similar" ignition-regime discharges of larger size and/or field. These discharges should be predictable apart from their relative differences in atomic processes such as neutral penetration, radiative loss, or possibly new transport processes resulting from α particles.

We can make a long but complete list of the dimensionless parameters starting with those based on geometry (safety factor q , aspect ratio R/a , elongation b/a), profiles (relative density- and temperature-gradient scale lengths L_n/a , L_T/a , and temperature ratios T_e/T_i), and atomic physics (working-gas atomic number, relative beam-heating penetration length, etc.). Apart from these, the remaining pure plasma parameters are plasma $\beta \propto nT/B^2$, collisionality $\hat{\nu} = (v_{ei}/c_s)a \propto na/T^2$, and relative ion gyroradius ρ_s/a (v_{ei} is the electron-ion collision frequency, $c_s = \sqrt{T/M}$, and $\rho_s = c_s/\Omega$, where $\Omega = eB/Mc$ is the gyrofrequency). We explicitly assume that quasineutrality applies so the relative Debye length λ_D/a is irrelevant. Discharges with all these dimensionless parameters identical can be called "dimensionally identical." It has been shown^{2,3} that dimensionally identical discharges have global confinement time scaled to the gyrofrequency: $\tau\Omega \propto \text{const}$ or $\tau \propto B^{-1}$ since the full nonlinear equations can be rescaled. While it has been argued⁴ that ignition tokamaks will have almost the same dimensionless parameters, it is not practical to scale dimensionally identical discharges to ignition.

However, it is possible to reach ignition by keeping all dimensionless parameters fixed save ρ_s/a . Such discharges can be called "dimensionally similar."

In this Letter, we will make the *theoretical* argument that the scaling of dimensionally similar discharges with respect to gyroradius should be very simple: All theories fall into two extremes, $\tau_{gB} \propto B^{-1}(\rho_s/a)^{-3} \propto Ba^{5/2}$ which we call gyro-Bohm-like (gB) or $\tau_B \propto B^{-1}(\rho_s/a)^{-2} \propto B^{1/3}a^{5/3}$ which we call Bohm-like (B). While nearly all theoretical models in use are gyro-Bohm-like, we show that direct *statistical analysis* of worldwide L -mode data on global confinement suggests a scaling slightly more pessimistic than Bohm: $\tau_{\text{emp}} \propto B^0 a^{1.8}$. However, we note that approximately correcting global gross confinement-time data for fast-ion storage and relative differences in beam-heating penetration indicates the underlying diffusion process may be gyro-Bohm-like. To resolve this discrepancy and uncertainty, we have performed a controlled *experiment* on the DIII-D tokamak. We have taken care to make and compare dimensionally similar discharges of the same size but different magnetic fields. While these L -mode discharges follow the conventional empirical scaling for global confinement time, standard transport analysis shows in a dramatic way that the magnetic-field scaling of heat diffusivity is best described by the gyro-Bohm-like scaling $\chi \propto 1/Ba^{1/2}$. Transport-code analysis shows that the deviation from the expected global scaling $\tau \propto a^2/\chi \propto Ba^{5/2}$ is due almost entirely to the difference in beam-heating penetration. Since a difference in heating profile can be technically controlled in principle (i.e., made self-similar), we believe the first steps to a rational "wind-tunnel"-like magnetic-fusion design principle and scaling law have been taken: $nT\tau \propto B^3 a^{5/2} \propto I^3/a^{1/2}$. This is far more optimistic than the present purely empirical fusion design scaling $nT\tau \propto B^2 a^{1.8} \propto I^2/a^{0.2}$. The actual attainment of improved global confinement and the more favorable size scaling remains to be confirmed experimentally.

Theory.—There appear to be two possible types of turbulent diffusion in a magnetized plasma depending on whether step or eddy size (Δ) scales to an intrinsic plasma parameter like the gyroradius or to the device size: microturbulence or macroturbulence. In either case, the diffusivity χ should be proportional to a rate (c_s/a)

$\times (\rho_s/\Delta)$ (essentially the diamagnetic frequency) and a step size squared, so that $\chi \propto (c_s/a)(\rho_s/\Delta)\Delta^2 F$, where F is a form factor containing possibly complicated dependences on the "similarity parameters" held fixed in dimensionally similar discharges as described above. We drop all further references to such form factors. With the similarity parameters fixed, all intrinsic plasma lengths can be scaled to ρ_s . If $\Delta \propto \rho_s$, we obtain the microturbulence or gyro-Bohm-like scaling, $\chi_{\text{gB}} \propto c_s \rho_s (\rho_s/a) \propto T^{3/2}/B^2 a$. For $\Delta \propto a$, we obtain the macro-turbulence or Bohm-like scaling, $\chi_{\text{B}} \propto c_s \rho_s \propto T/B$. Keeping β and collisionality fixed, $n \propto B^{4/3} a^{-1/3}$, $T \propto B^{2/3} a^{1/3}$, and $\rho_s/a \propto B^{-2/3} a^{-5/6}$. Thus, $\chi_{\text{gB}} \propto B^{-1} a^{-1/2}$ and $\chi_{\text{B}} \propto B^{-1/3} a^{1/3}$. If radiation losses and heating profiles are kept self-similar, then we can assume $\tau \propto a^2/\chi$ and obtain $\tau_{\text{gB}} \propto B a^{5/2}$ and $\tau_{\text{B}} \propto B^{1/3} a^{5/3}$. As we shall emphasize, this latter assumption commonly breaks down in practice.

Proof by example may be more convincing. Note that all collisional or neoclassical diffusion processes are gyro-Bohm-like. All electrostatic-drift-wave modeling formulas commonly used for fitting and projecting to ignition assume wavelengths scaled to ρ_s (e.g., Ref. 5). In the present context, these may be seen as providing interpolation formulas for F . However, the gyro-Bohm-like scaling is not limited to $\mathbf{E} \times \mathbf{B}$ electrostatic-drift-wave transport. It also includes formulas for magnetic transport from microtearing modes (similar to $\mathbf{E} \times \mathbf{B}$ collisional-drift-wave scaling) and electromagnetic transport at very short wave (c/ω_{pe}) scales (e.g., Ohkawa-type⁶ models). Nearly all theoretical models in current use are in fact gyro-Bohm-like. There are few Bohm-like examples. We can only cite the recent suggestion from simulations of resistive magnetohydrodynamic (MHD) turbulence⁷ that dominant wave numbers scale to lowest n . This leads to a mixed, nearly Bohm scaling $\chi \propto c_s \rho_s (\rho_s/a)^{1/3}$ for similarity parameters fixed.

A cautionary note on the testing and application of dimensionally similar discharges is needed. One must stay well within the operational density limits. It is believed that this is at least bounded by the radiation-collapse limit scaling as $n_{\text{limit}} \propto (B/Rq)(P/P_{\text{OH}})^{1/2}$ (e.g., Ref. 5). The Ohmic-heating power scales as $P_{\text{OH}} \propto B a^{1/2}$ as does the total power to sustain gyro-Bohm confinement along a similarity path. In contrast, for Bohm confinement $P = B^{5/3} a^{4/3}$. Combining with the density scaling, $n/n_{\text{limit}} \propto B^{1/3} a^{2/3}$ for gyro-Bohm and $B^{2/3} a^{1/6}$ for Bohm scaling. Since n/n_{limit} must be less than unity, the scaling range is limited. Furthermore, the relative T_i/T_e equilibration rate τ_E/τ_{eq} must increase in a dimensionally similar scan. Thus, the scan (or projection) should start with equilibrated discharges so T_i/T_e does not change.

Statistical analysis.—While the preponderance of theoretical models favor gyro-Bohm scaling of diffusion coefficients, superficial statistical analysis of global confinement-time data has heretofore indicated a Bohm-

like scaling or worse. To determine the gyroradius scaling, $\tau \propto B^{-1}(\rho_s/a)^{\alpha_1}$, we must do a standard statistical regression¹ with respect to all variables to determine α_1 . Under the single constraint of plasma physics,³

$$\tau \propto B^{-1}(\rho_s/a)^{\alpha_1}(\hat{v})^{\alpha_2}\hat{\beta}^{\alpha_3}q^{\alpha_4}(R/a)^{\alpha_5}(b/a)^{\alpha_6}A^{\alpha_7}. \quad (1)$$

(Here we have used the variable $\hat{\beta} = \beta/\beta_{\text{crit}}$, where $\beta_{\text{crit}} = 3.5I/aBq_0 \propto a/Rq$.) ρ_s/a , \hat{v} , and $\hat{\beta}$ depend on the temperature T which can be obtained from the machine variable P , the power deposited, via the relation $\tau \propto nTa^3(R/a)(b/a)/P$. One can use a temperature form for these dimensionless plasma variables or rewrite them directly in terms of power.⁸ The power form gives less scatter. The dimensionally constrained fit in terms of machine variables follow algebraically:

$$\tau \propto B^{\beta_0} a^{\beta_1} P^{\beta_2} n^{\beta_3} q^{\beta_4} (R/a)^{\beta_5} (b/a)^{\beta_6} A^{\beta_7}. \quad (2)$$

The power form of the dimensionless variables fitted to a large L -mode confinement-time database (1988 updated Kaye database; Ref. 1) gave the result $\alpha_1 = -1.94$, $\alpha_2 = -0.236$, $\alpha_3 = -0.624$, $\alpha_4 = -1.33$, $\alpha_5 = -0.556$, $\alpha_6 = 1.48$, and $\alpha_7 = 0.500$, corresponding to $\beta_0 = 1.03$, $\beta_1 = 2.39$, $\beta_2 = -0.529$, $\beta_3 = 0.123$, $\beta_4 = -0.923$, $\beta_5 = -0.027$, $\beta_6 = 1.22$, and $\beta_7 = 0.500$. The result is very close to the original Goldston⁹ L -mode fit $\tau \propto IP^{-1/2} n^0 a^{-0.37} R^{1.75}$ which we shall refer to as *the* empirical scaling. One might conclude that transport is Bohm-like ($\alpha_1 = -2$) or worse.

However, this procedure is strongly skewed by the effects of fast-ion storage and the parametric variation of the beam-heating penetration illustrated in Fig. 5 of Ref. 10. Both effects tend to decrease the total stored energy confinement time with increasing density. Correction for fast-ion storage is relatively straightforward. To approximately correct for beam penetration, we can attempt to normalize the experimental discharge confinement time from each machine to what it should have been with penetration corresponding to a fixed reference density for each machine. However, this procedure is somewhat dependent on the diffusion model and the choice of reference density. Nevertheless, making these approximate corrections so as to obtain a better estimate of the underlying diffusion scaling, we find power-form fits very close to pure gyro-Bohm ($\alpha_1 = -3.00$) scaling; also the resulting favorable density dependence is $\beta_3 = 0.60$ (in place of $\beta_3 = 0.123$). Christiansen, Cordey, and Thomsen¹¹ have statistically analyzed JET L - and H -mode data in terms of gyro-Bohm- and Bohm-like forms. Correcting for fast ions, they concluded that gyro-Bohm fits were somewhat better.

It should be noted that no beam-heating corrections are needed in the case of Ohmic heating. At low density, the well-known neo-Alcator scaling prevails. While it is likely that the diffusion mechanisms are different from those governing the L mode (e.g., Ref. 5), we can show that the diffusion is nearly gyro-Bohm-like. Taking the dimensionally constant fit $\tau \propto n a^{5/4} R^2 (P/P_{\text{OH}})^{\gamma}$ and projecting along a similarity path gives $\tau \propto B^{1.33} a^{3.08}$,

which is clearly closer to gyro-Bohm diffusion $B^{1.00}a^{2.5}$ than Bohm $B^{0.33}a^{1.66}$.

Experiment.—To better resolve the apparent discrepancy between the preponderance of gyro-Bohm diffusion theories and superficially Bohm-like scaling of gross empirical confinement time, we carried out a controlled experiment on DIII-D. *L*-mode discharges of fixed size $a=65$ cm, aspect ratio $R/a=2.7$, elongation $b/a=1.70$, and $q=3.8$ were compared at $B=1.05$ T (1 MA) and $B=2.1$ T (2 MA) keeping β and collisionality fixed. The 1-T reference discharge was established at $\bar{n}_e=3.8 \times 10^{13}$ cm $^{-3}$ with 3.7 MW of total power (0.36 MW Ohmic heating). It had a reactor-relevant $\langle\beta\rangle_{th} \approx 1.9\%$ ($\beta/\beta_{crit} \approx 0.35$) with $v_{*}^{min}=0.13$. By adjusting the gas speed, the 2-T discharge was at $\bar{n}_e=9.6 \times 10^{13}$ ($2^{4/3}$ times the reference density). 16 MW of total power was required to nearly quadruple the stored thermal energy from 0.35 to 1.29 MW. For this discharge $\langle\beta\rangle$ and v_{*}^{min} were unchanged. The Z_{eff} profile was nearly constant at 1.5 to 1.6 and nearly the same in each case. The electron and ion temperatures were near-

ly equilibrated in both discharges and we have lumped the measurements together in a single temperature. $T(0)$ increased from 1.89 to 2.75 keV or 1.46 times. This is close to the similarity ratio $2^{2/3}=1.587$. $n_e(0)$ increased from 5×10^{13} to 12×10^{13} cm $^{-3}$ or 2.4 times. This is close to the similarity ratio $2^{4/3}=2.51$. Figure 1 compares the measured temperature and density profiles for the 2- and 1-T cases. The dashed lines represent the 1-T profiles normed to the 2-T central values illustrating that they are nearly similar. It should be made clear that scaling over a wider range (say, 0.7–2.1 T) would be difficult. The high density is already limited by the usual radiation collapse and operation at lower density is limited by so-called “locked modes” as well as the lack of T_e and T_i equilibration.

The gross confinement followed the expected *L*-mode empirical scaling and remained almost constant: 97 to 81 msec or a 17% decrease, whereas the empirical $\tau \propto In^0/P^{1/2}$ predicts only a 4% drop. The global thermal confinement time was also nearly constant: 82 to 72 msec. However, despite the near constancy or even degradation of the total confinement time, the local heat diffusivity was best described by a $1/B$ scaling. Standard transport-code analysis was used to calculate $\chi(r)$ from the experimental density and temperature profiles and the known profile of transport power flow

$$P_{tr}(r) = P_{beam}(r) + P_{OH}(r) - P_{rad}(r) - P_{conv}(r) : -2n(r)\chi(r)\partial T/\partial r = \rho P_{tr}(r)/S(r), \quad (3)$$

where r is the volume radius normed to the total volume radius ρ and $S(r)$ is the surface area [$\chi \equiv (n_e\chi_e + n_i\chi_i)/(n_e + n_i)$, $n = (n_e + n_i)/2$]. The beam power flow $P_{beam}(r)$ is thought to be well calculated, the radiation loss $P_{rad}(r)$ was measured, and the Ohmic power $P_{OH}(r)$ and convective flow $P_{conv}(r)$ were not significant. Figure 2 shows the ratio of the 2- and 1-T χ values (χ_2/χ_1) versus the volume radius. Over the inner 95% of the discharge, χ behaves in a nearly gyro-Bohm-like fashion,

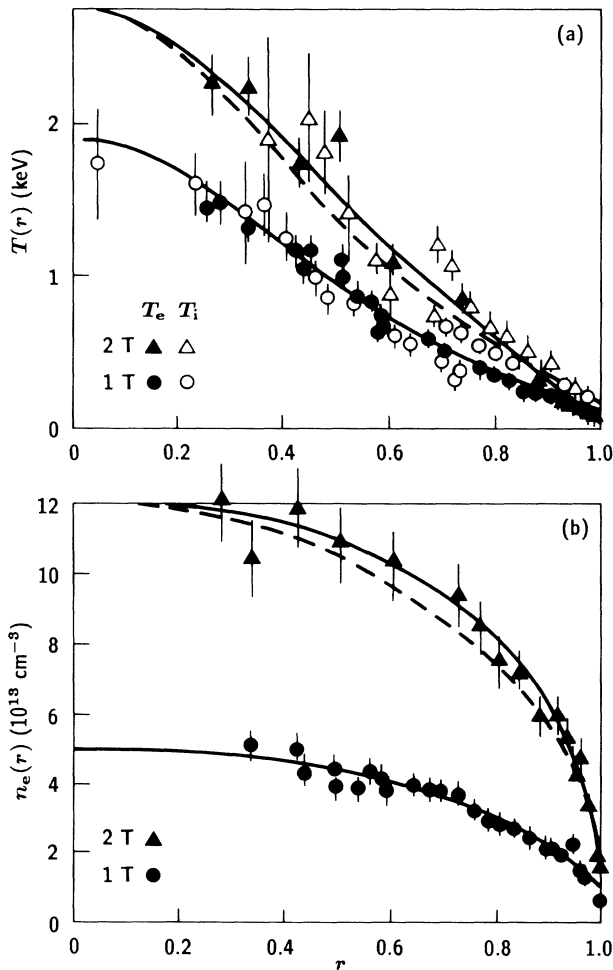


FIG. 1. (a) Temperature and (b) density profiles at 1 and 2 T (solid lines) vs normed volume radius r . 1-T profiles normed to 2-T central values (dashed lines).

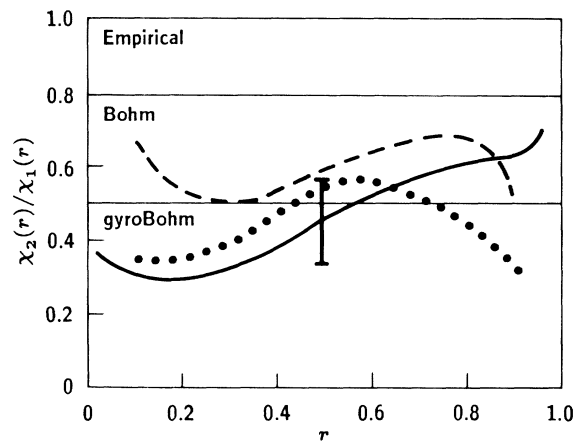


FIG. 2. Ratio of 2- and 1-T average heat diffusivity vs normed volume radius (solid line). Ratio of heat diffusivities normed to inverse temperature (dotted line) and density- (dashed line) gradient lengths.

i.e., $\chi_2/\chi_1 \approx \frac{1}{2}$. We cannot, however, rule out Bohm-like processes localized to the edge. Since χ in most theories is inversely proportional to the plasma gradient lengths and these were not strictly constant, we also show the ratios of χL_n (dashed line) and χL_T (dotted line). We can still conclude that $\chi \propto 1/B$ times some radial variation arising from the radial variation of the similarity variables. Absolute errors in χ measurements combining electron and ion channels for equilibrated temperatures are typically 20%. If these errors are statistically independent with no allowance for cancellation of systematic errors, the relative error in χ_2/χ_1 is 28%, indicated in the figure.

To understand why the global confinement time had the pessimistic $\tau \propto B^0$ scaling whereas the heat diffusivity was consistent with an optimistic $\chi \propto 1/B$ scaling, it must be remembered that global confinement depends on the heating process as well as the diffusion process. The neutral-beam-heating process is less efficient at high density where it tends to deposit more power at the edge relative to the center. Figure 3(a) shows the normalized profiles of the beam power flows (solid lines) and the transport power flows (dashed lines). Clearly, the heating profiles were not similar in the 1- and 2-T cases. Figure 3(b) shows the transport confinement time as a function of normed volume radius $\tau_{tr}(r)$ for the 1- and 2-T cases (solid lines). [$\tau_{tr}(r) = W(r)/P_{tr}(r)$, where $W(r)$ is the energy stored inside r .] As we have already noted, the global values are nearly the same: $\tau_{tr_2}(1) \approx \tau_{tr_1}(1)$. However, the central values of τ_{tr} are considerably larger in the 2-T case as compared to the 1-T case since the power deposited to the center was relatively small. To verify that the poor confinement-time scaling is actually consistent with a gyro-Bohm diffusion scaling, we can solve the transport equation [Eq. (3)] for temperature using the 2-T density $n(r)$ and the 2-T transport power [$P_{tr}(r)$] but with $\chi(r) = \frac{1}{2} \chi_1(r)$, i.e., according to perfect gyro-Bohm scaling. The resulting temperature can be used to compute $\tau_{tr}(r)$. As shown by the dashed line, it is nearly the same as the 2-T experimental curve and, in particular, reproduces the poor global confinement. [Similarly, the 1-T $\tau_{tr}(r)$ curve is approximately reproduced by using the 1-T $n(r)$ and $P_{tr}(r)$ with $\chi(r) = 2\chi_2(r)$.] It also follows from Eq. (3) that if $n_2(r) \equiv 2^{4/3} n_1(r)$, $\chi_2(r) \equiv \frac{1}{2} \chi_1(r)$, and $P_{tr_2}(r) = 2P_{tr_1}(r)$, then $T_2(r) \equiv 2^{2/3} T_1(r)$ and $\tau_{tr_2}(r) \equiv 2\tau_{tr_1}(r)$; i.e., gyro-Bohm global confinement-time scaling can result only if the heating profiles are also similar.

In summary, our B -scaling experiment has shown that the diffusion process has a gyro-Bohm scaling $\chi \propto 1/B$ for dimensionally similar discharges from which we can infer $\chi \propto 1/a^{1/2}$ for size scaling. Further, we can predict that if confinement experiments are scaled with self-similar heating profiles, then the ignition parameter should scale as $nT\tau \propto B^3 a^{5/2}$ (gyro-Bohm-like) rather than $nT\tau \propto B^{7/3} a^{5/3}$ (Bohm-like) or the "standard" empirical relation $nT\tau \propto B^2 a^{1.8}$.

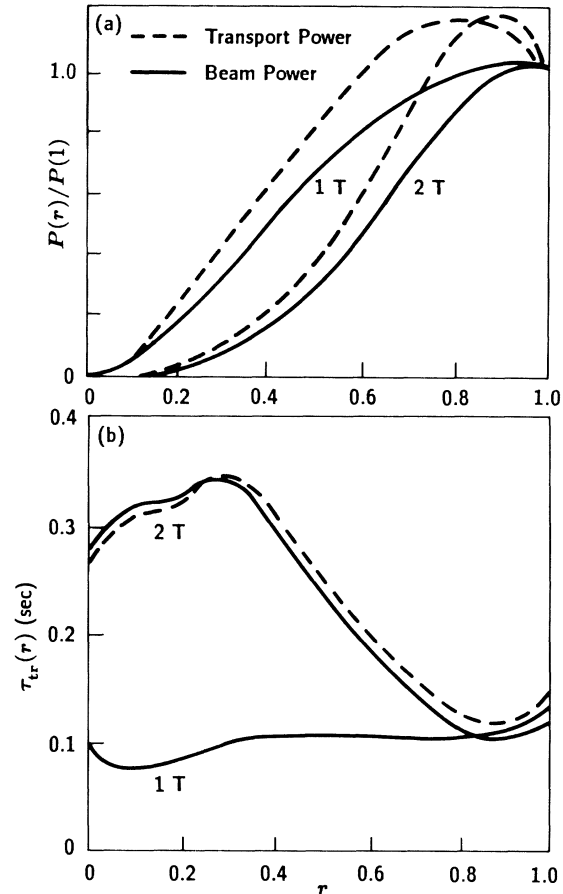


FIG. 3. (a) Normalized power flows vs volume radius. (b) Experimental transport confinement time vs normed volume radius (solid line). Projected 2-T transport confinement time using one-half the 1-T heat diffusivity (dashed line).

This work was sponsored by the U.S. Department of Energy under Contract No. DE-AC03-89ER51114.

(a) Also at University of California at San Diego, La Jolla, CA 92093.

¹S. Kaye, Phys. Fluids **28**, 2327 (1985).

²B. B. Kadomtsev, Fiz. Plazmy **1**, 531 (1975) [Sov. J. Plasma Phys. **1**, 295 (1975)].

³J. W. Connor and J. B. Taylor, Nucl. Fusion **19**, 1047 (1977); Plasma Phys. Controlled Fusion **30**, 619 (1988).

⁴J. Sheffield, Oak Ridge National Laboratory Report No. ORNL/P-90/0979, 1990 (to be published).

⁵R. E. Waltz, R. R. Dominguez, and F. W. Perkins, Nucl. Fusion **29**, 351 (1989).

⁶T. Ohkawa, Phys. Lett. **67A**, 35 (1978).

⁷B. A. Carreras and P. H. Diamond, Phys. Fluids B **1**, 1011 (1989).

⁸R. Bickerton, University of Texas at Austin Report No. FRCR 374, 1990 (unpublished).

⁹R. J. Goldston, Plasma Phys. Controlled Fusion **26**, 87 (1984).

¹⁰R. R. Dominguez and R. E. Waltz, Nucl. Fusion **27**, 65 (1987).

¹¹J. P. Christiansen, J. G. Cordey, and K. Thomsen, Nucl. Fusion **30**, 1183 (1990).